

New generation of precast concrete double tees reinforced with carbon-fiber-reinforced polymer grid

Dillon Lunn, Gregory Lucier, Sami Rizkalla, Ned Cleland, and Harry Gleich

Precast, prestressed concrete double tees are commonly used in buildings and parking structures. The stems of these members are prestressed longitudinally for flexure and are reinforced with vertical stirrups or welded-wire reinforcement (WWR) to resist the applied shear. Transverse reinforcement in the top flange is traditionally provided by WWR. While WWR is safe and effective from a structural perspective, it is vulnerable to corrosion. Parking garages can be harsh environments for steel reinforcement, particularly the reinforcement in the wearing surface of the double-tee deck flange. Small-diameter strands of fiber-reinforced polymer (FRP) are available in a grid configuration and have been used to replace traditional WWR transverse flange reinforcement in double-tee members. FRP grid has several advantages in comparison with traditional WWR, including high strength, corrosion resistance, light weight, and ease of installation.

It has been a common assumption that the design of double-tee-flange reinforcement is governed by the concentrated load of 3000 lb (13 kN) prescribed by ASCE/SEI 7–10.¹ An earlier research program demonstrated that much larger portions of double-tee flanges than commonly assumed act to resist bending from concentrated loads, both in the vicinity of flange-to-flange connections and away from them.² That result showed that double-tee-flange design is governed by the uniform load criteria for parking live load and other superimposed uniform loads.

This paper summarizes research undertaken to evaluate the behavior, serviceability, and failure mode of double-tee flanges reinforced with carbon-fiber-reinforced polymer (CFRP) grid under uniform applied load. Based on the observed behavior and measured response, design recommendations have been developed.

Experimental program

The research included an extensive experimental program, which comprised testing eight short double-tee beams,

- Double-tee flanges reinforced with fiber-reinforced polymer (FRP) grid were subjected to uniform gravity pressure to examine their serviceability and failure mode.
- The mode of failure for these specimens was governed by the tensile strength of the concrete, with concrete cracking followed immediately by rupture of the FRP grid.
- It is recommended that the reduced nominal flexural strength with a strength-reduction factor ϕ of 0.75 exceed the moment due to factored load and that the reduced cracking moment capacity exceed 1.33 times the moment due to factored load.

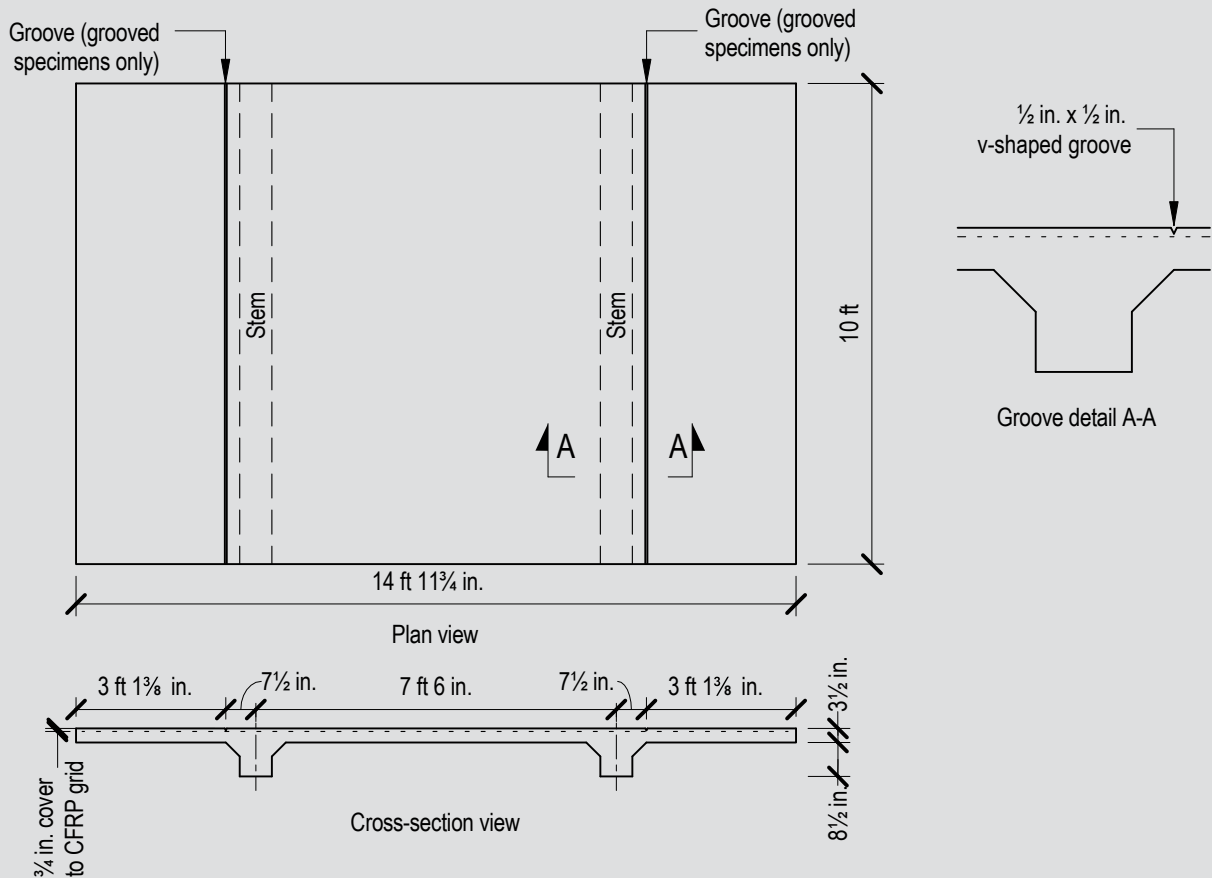


Figure 1. Test-specimen details (longitudinal reinforcement not shown). Note: 1 in = 25.4 mm; 1 ft = 0.305 m.

each measuring 15 × 10 ft (4.6 × 3 m) with a flange thickness of 3.5 in. (90 mm). Two tests were conducted on each of the eight specimens (one test on each flange cantilever) for a total of 16 full-scale tests of the flange. **Figure 1** depicts a schematic of the test specimen. The depth of the stem in the test specimens was reduced because the research focused on the behavior of the flange. The height of the stems was 12 in. (300 mm), including the 3.5 in. thickness of the flange. Two types of CFRP grid were investigated: C50 × 2.7 with a grid spacing of 2.7 in. (69 mm), and C50 × 3.9 with a grid spacing of 3.9 in. (99 mm). The C of the C50 designation indicates carbon fibers, and the 50 indicates the relative size of the strands. For example, C100 has roughly twice the cross-sectional area of C50 strand. Variation of the grid spacing was investigated to determine the effectiveness of the CFRP grid with respect to the flexural strength of the flange. The study also included the effect of a reduced-thickness flange at the maximum moment location. A V-shaped groove was tooled into the top surface of four of the specimens to the depth of the transverse FRP reinforcement at the maximum moment section of the cantilever. The tooled grooves enabled study of flange behavior without a significant contribution from the concrete in tension (Fig. 1). In some cases, the actual groove depth was slightly less than the depth of the reinforcement. The measured concrete compressive strength

f'_c of the test specimens varied between 7050 psi (48.6 MPa) and 8140 psi (56.1 MPa), with an average strength of 7800 psi (53.8 MPa). **Table 1** provides the measured material properties of the C50 carbon grid.

All specimens were subjected to a uniformly distributed pressure up to failure using a vacuum chamber. To study the behavior under sustained loads, four specimens were subjected to the factored load for 24 hours and the remaining specimens were subjected to the factored load for one hour. To increase the number of tests, one flange cantilever was propped while the other was tested. After failure of the unsupported cantilever flange, the props were removed

Table 1. CFRP grid properties (provided by the grid manufacturer)

Property	Value
Tensile modulus of elasticity E_f , ksi	34,000
Individual strand cross-sectional area, in. ²	0.00286
Strand tensile strength, lb (2.7 in. spacing)	1218
Strand tensile strength, lb (3.9 in. spacing)	1210

Note: CFRP = carbon-fiber-reinforced polymer. 1 in. = 25.4 mm; 1 lb = 4.448 N; 1 ksi = 6.895 MPa.

Table 2. Test program

Specimen	Test	Grid spacing	Thickness at critical section	Duration of hold under factored design loading, hr	Flange supports		
					Left	Center	Right
1	1.A	2.7	Full thickness	24	Free	Free	Propped [†]
	1.B				n/a	Propped [†]	Free
2	2.A			1	Free	Free	Propped
	2.B				n/a	Propped	Free
3	3.A		Grooved	24	Free	Free	Propped [†]
	3.B				n/a	Propped [†]	Free
4	4.A			1	Free	Free	Propped
	4.B				n/a	Propped	Free
5	5.A	3.9	Full thickness	24	Free	Free	Propped [†]
	5.B				n/a	Propped [†]	Free
6	6.A		1	Free	Free	Propped	
	6.B			n/a	Free	Free	
7	7.A	Grooved	24	Free	Free	Propped [†]	
	7.B			n/a	Propped [†]	Free	
8	8.A		1	Free	Free	Propped	
	8.B			n/a	Propped	Free	
8.0*	8.B.0				n/a	Propped	Free

Note: n/a = not applicable. 1 in. = 25.4 mm;

* Remaining portion of original damaged specimen

[†] Propped in place after 24-hour hold completed

from the opposite cantilever and repositioned to support the center span between the two stems prior to testing the second cantilever flange to failure. One exception to this scheme was that specimen 6B was tested without propping the center span. **Table 2** gives a summary of the testing program.

Test setup and methodology

A specimen, its supports, and the required instrumentation were placed inside the vacuum chamber and the top of the chamber was sealed with plastic, leaving the top surface of the specimen free to deform. The pressure in the chamber was reduced using a modified industrial blower, generating uniform pressure on the top surface of the flange of the double tee.

Figure 2 shows schematics of the concept used to apply external uniform pressure. At the start of the test, the pressure outside the chamber P_1 and the pressure inside

the chamber P_2 are both equal to atmospheric pressure; thus no load is applied on the top surface of the double-tee flange. When the blower is activated, P_2 is reduced while P_1 remains constant. With P_1 greater than P_2 , the atmosphere presses evenly inward on the rigid walls of the chamber and on the top surface of the double tee. A small gap (nominal 1.5 in. [40 mm]) was maintained between the edges of the double-tee flange and the chamber walls to maintain a uniform load distribution on the double tee.

Each double-tee specimen was supported along the length of its two stems by wooden blocks resting on concrete blocks. Screw jacks were used to prop the right cantilever flange while the left cantilever flange was tested (Fig. 2). After failure of the left flange, the damaged flange was removed, and a wooden table was used to fill the empty space. The screw jacks were moved from the right cantilever flange to the center span, and the right cantilever flange was then tested (Fig. 2).

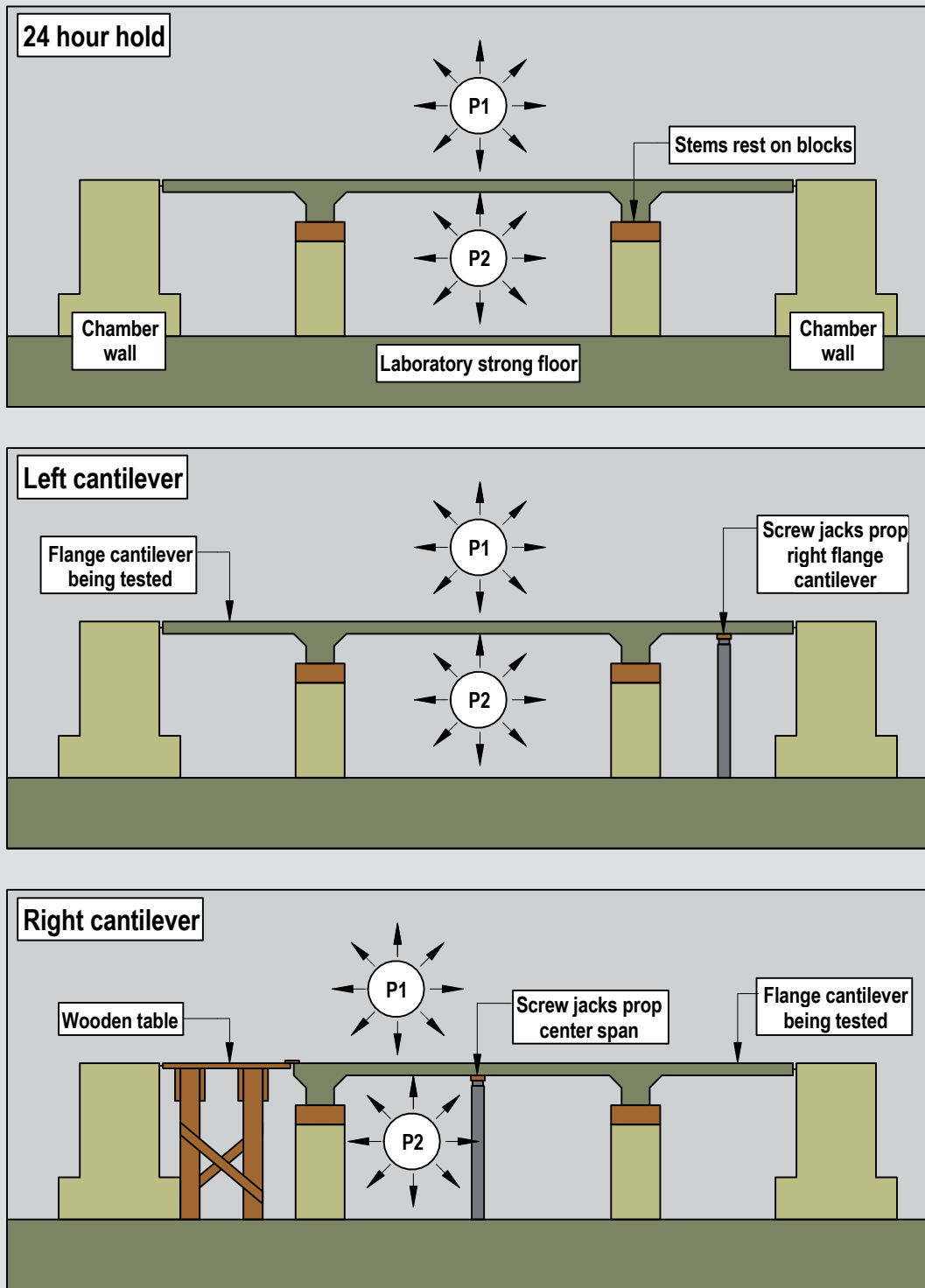


Figure 2. Test configurations. Note: $P1$ = pressure outside testing chamber; $P2$ = pressure inside testing chamber.

Two sides of the chamber consisted of reinforced concrete inverted-tee girders that were post-tensioned to the laboratory strong floor. The other walls of the chamber consisted of steel wide-flange girders (with heavy stiffener plates) spanning between the two concrete girders and supporting

wooden planks (**Fig. 3**). The chamber was designed to be rigid and to withstand the applied pressure with insignificant deformation. Gaps along the base of the chamber and the strong floor of the laboratory were sealed using caulk and expanding foam to minimize air leakage.

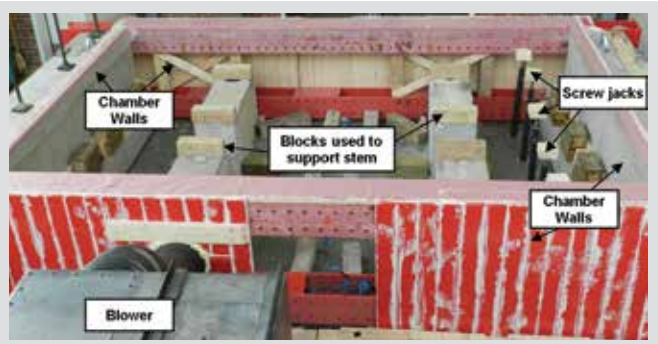


Figure 3. Vacuum chamber before testing.

$$= 1.2(43.75) + 1.6(40) + 0.5(20)$$

$$= 126.5 \text{ lb/ft}^2 \text{ (6.06 kPa)}$$

Crack patterns and failure modes

The specimens were designed for a live load L of 40 lb/ft² (2 kPa) and a snow load S of 20 lb/ft² (1 kPa). The controlling factored load combination based on ASCE/SEI 7-10,¹ including the dead load D , was determined as $1.2D + 1.6L + 0.5S$. The dead load considered was the weight of the flange only. Specimens were loaded and unloaded in incremental cycles to failure.

Applied pressure, deflections, and primary crack widths were monitored throughout testing. The applied pressure was measured using a pressure transducer. String potentiometers were used to measure vertical displacements of the double-tee specimens. Thirteen string potentiometers were used in testing the left cantilever flange (test A), whereas only four potentiometers were used for the right cantilever flange (test B). For specimens subjected to a 24-hour hold under factored loading, crack opening displacement was measured using four linear potentiometers. The linear potentiometers were centered above the critical sections on either side of the stem adjacent to the left cantilever flange. For the right cantilever flange, linear potentiometers were moved to the corresponding locations adjacent to the right stem. This location was selected to measure the crack on the interior and exterior side of the stem.

Test results

All specimens resisted an applied pressure greater than the factored design pressure prior to failure. **Table 3** provides a summary of the measured values, including the pressure causing the first crack and the pressure at failure. The table also provides the ratio of the measured pressure at failure to the factored design pressure and the location of the failure. The measured pressure at first cracking was determined as the pressure at which a significant change in the slope of the load-deflection response occurred. Many of the specimens, especially those with a tooled groove, did not exhibit this change in slope prior to failure. The measured pressure at first crack and at failure included the self-weight of the flange, which is 43.75 lb/ft² (2.09 kPa). The factored design load q_u was determined using Eq. (1).

$$q_u = 1.2D + 1.6L + 0.5S \quad (1)$$

Figure 4 shows the typical failure mode of the left cantilever flange. Failure occurred immediately following initiation of the crack for both the full-thickness and grooved specimens in the tension zone. Rupture of the CFRP grid immediately followed cracking of the concrete. No crushing of the concrete was observed on the compression side of the double-tee specimens. All specimens with the exception of two full-thickness specimens with 3.9 in. (99 mm) grid spacing (5B and 6B) failed on the exterior side of the stem at a location directly above the edge of the stem chamfer. Specimen 5B failed after cracking on the interior side of the stem. Specimen 6B was not propped at the center span between the stems; and, as a result, failed at approximately 34 in. (870 mm) from the edge of the stem, corresponding to the location of maximum positive moment.

All of the grooved specimens except specimen 4A, which had a 2.7 in. (69 mm) grid spacing, failed immediately after initiation of the crack at the exterior side of the stem. All full-thickness specimens except specimen 6, which had a 3.9 in. (99 mm) grid spacing, cracked prior to failure at the interior side of the stem, with failure occurring immediately after initiation of the crack at the exterior side of the stem.

Ultimate strength

Measured pressure at failure (including the dead load) of the double-tee flanges varied between 222 lb/ft² (10.6 kPa) and 347 lb/ft² (16.6 kPa) (**Fig. 5**). **Table 4** provides the average measured pressure, standard deviation, and average ratio of the measured pressure at failure to the factored design pressure for each of the four types of specimens. The ratios vary from 1.90 to 2.02 for the grooved specimens and from 2.59 to 2.66 for full-thickness specimens. The measured failure pressure for all tested specimens corresponds to the cracking moment resistance of the flange, which is reduced for the grooved specimens due to the reduced thickness of the flange. The measured pressure at failure was not sensitive to the type of grid used, but rather appeared to relate to the tensile strength of the concrete. Immediate failure occurred after cracking and prior to development of the full strength of the CFRP grid.

Vertical deflections

All measured deflections at service load were less than 0.04 in. (1 mm). The measured net deflection at ultimate varied between 0.06 and 0.78 in. (1.5 and 20 mm) and was highly dependent on the location of cracks prior to failure (**Fig. 6**). The significant increase in deflection

Table 3. Summary of results

Test	Grid Spacing, in.	Thickness at critical section	Measured pressure* at first crack P_{cr} , lb/ft ²	Measured pressure* at failure P_{exp} , lb/ft ²	Ratio of failure pressure to the factored design pressure	Failure location
1.A	2.7	Full thickness	282	338	2.67	Fixed end of cantilever
1.B			316	326	2.58	
2.A			204	337	2.66	
2.B			290	345	2.73	
3.A		Grooved	283	283	2.23	Fixed end of cantilever
3.B			248	248	1.96	
4.A			199	255	2.01	
4.B			237	237	1.88	
5.A	3.9	Full thickness	310	347	2.75	Fixed end of cantilever
5.B			339	345	2.73	Flange between stems
6.A			318	318	2.51	Fixed end of cantilever
6.B			300	300	2.37	Flange between stems
7.A		Grooved	254	254	2.01	Fixed end of cantilever
7.B			265	265	2.09	
8.A			233	233	1.84	
8.B			222	222	1.76	
8.B.0			227	227	1.80	

Note: 1 in. = 25.4 mm; 1 lb/ft² = 0.04788 kPa.

*Includes self-weight of 43.8 lb/ft².

before failure for the full-thickness specimens was due to the initiation of a crack at the interior side of the stem, followed by the formation of another crack on the exterior side of the stem, which led to failure. The average deflection for full-thickness specimens was nearly five times the average deflection of grooved specimens. **Figure 7** shows the behavior of the full-thickness specimens. The typical initial crack occurred at the interior side of the stem, caus-

ing a sudden and large deflection; however, the specimen was able to carry additional load and deflect further until cracking occurred on the exterior side of the stem, causing failure. The grid spacings selected did not significantly affect the load-deflection behavior for the full-thickness or grooved specimens.

Discussion

Concrete tensile strength

Test results were used to determine the tensile strength of the concrete at failure. For full-thickness specimens, the total thickness of the flange was 3.5 in. (90 mm), whereas for grooved specimens, the thickness at the critical section was 3.0 in. (75 mm). **Figure 8** shows the tensile strength of the concrete at failure expressed as a function of the square root of the concrete compressive strength f'_c for each specimen. Test results indicate that the modulus of rupture exceeded the value of $7.5 \sqrt{f'_c}$ psi ($0.62 \sqrt{f'_c}$ MPa)



Figure 4. Typical failure of left flange cantilever.

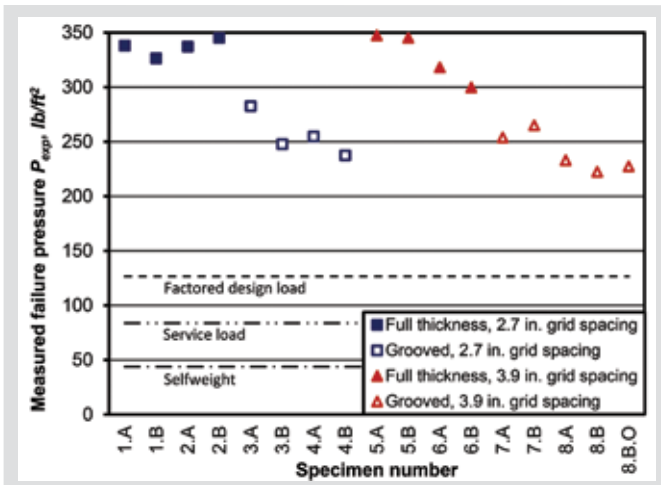


Figure 5. Measured failure pressure P_{exp} lb/ft². Includes self-weight.
Note: 1 in. = 25.4 mm; 1 lb/ft² = 0.0479 kPa.

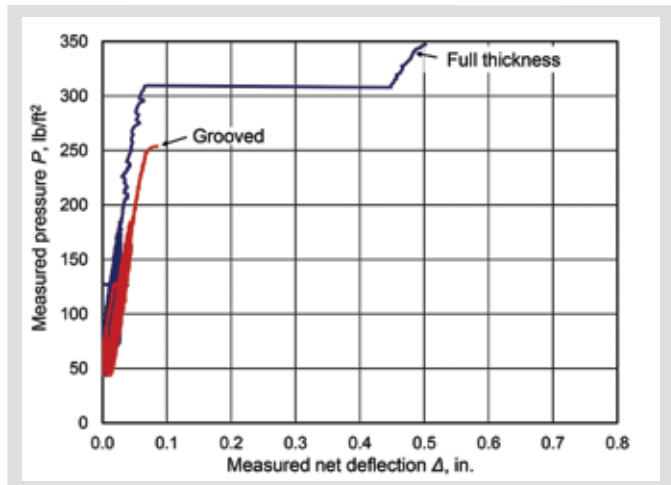


Figure 6. Typical load deflection for grooved and full-thickness specimens.
Note: 1 in. = 25.4 mm; 1 lb/ft² = 0.0479 kPa.

with the exception of specimen 6B. Failure of specimen 6B was in positive bending between the stems. Test results indicate that the average modulus of rupture for the majority of specimens was in the vicinity of $9.0\sqrt{f'_c}$ psi ($0.74\sqrt{f'_c}$ MPa) and was not dependent on the tooled groove or the reinforcement ratio. This result is consistent with the observation that failure initiated with tensile cracking of the concrete followed immediately by rupture of the CFRP grid reinforcement. This result is also consistent with splitting tension tests conducted on concrete cylinders that indicated the average tensile strength of the concrete to be $8.3\sqrt{f'_c}$ psi ($0.69\sqrt{f'_c}$ MPa).

Ultimate strength

The measured ultimate flexural strength for each flange was analyzed using the method recommended by ACI 440.1R-06.³ The predicted failure mode was determined by comparing the FRP reinforcement ratio ρ_f , as defined by Eq. (8-2),³ with the balanced FRP reinforcement ratio ρ_{fb} given in Eq. (8-3).³ If the FRP reinforcement ratio is less than the balanced ratio, then failure is likely to occur due to rupture of the FRP before crushing of the concrete. In this case, a simplified method and a conservative method recommended by ACI 440.1R-06 were used to determine

the nominal moment capacity M_n (Eq. [8-6b]).³

$$\rho_f = \frac{A_f}{bd} \quad (\text{ACI 8-2})$$

where

A_f = cross-sectional area of FRP reinforcement

b = width of critical section

d = effective depth of reinforcement

$$\rho_{fb} = 0.85\beta_1 \frac{f'_c}{f_{fu}} \frac{E_f \varepsilon_{cu}}{E_f \varepsilon_{cu} + f_{fu}} \quad (\text{ACI 8-3})$$

where

β_1 = factor relating depth of equivalent rectangular compressive stress block to neutral axis depth as specified by ACI 318-11

f_{fu} = rupture stress of FRP reinforcement

E_f = modulus of elasticity of FRP reinforcement

ε_{cu} = concrete crushing strain

Table 4. Average ultimate strength

Grid spacing, in.	Thickness at critical section	Average measured failure pressure* P_{exp} lb/ft ²	Standard deviation of measured failure pressure, lb/ft ²	Average ratio of failure pressure to factored pressure
2.7	Full thickness	337	7.9	2.66
	Grooved	256	19.6	2.02
3.9	Full thickness	328	22.6	2.59
	Grooved	240	18.5	1.90

Note: 1 in. = 25.4 mm; 1 lb/ft² = 0.04788 kPa.

*Includes self-weight of 43.8 lb/ft².

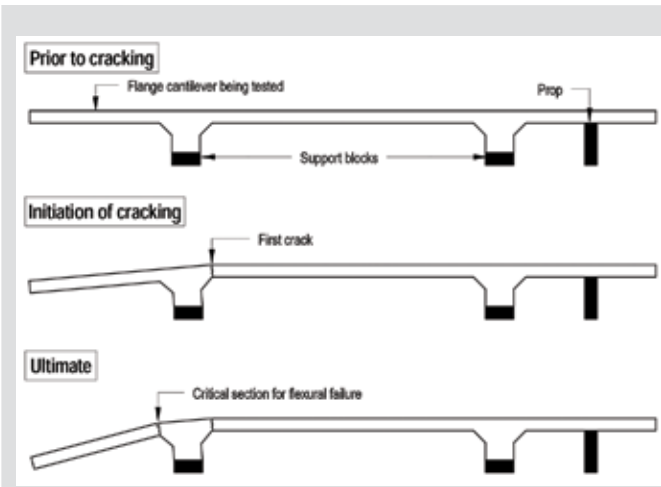


Figure 7. Typical behavior for full-thickness specimens.

$$M_n = A_f f_{fu} \left(d - \frac{\beta_1 c_b}{2} \right) \quad (\text{ACI 8-6b})$$

where

c_b = distance from the extreme compression fiber to the neutral axis at the balanced strain condition as determined by Eq. (8-6c)

$$c_b = \left(\frac{\epsilon_{cu}}{\epsilon_{cu} + \epsilon_{fu}} \right) d \quad (\text{ACI 8-6c})$$

where

ϵ_{fu} = design rupture strain of FRP reinforcement

It is also possible for failure to occur due to cracking of the concrete in tension if the cracking moment M_{cr} exceeds the nominal flexural moment corresponding to the tensile rupture strength of the FRP M_n . The cracking moment M_{cr} can be determined using Eq. (2). The experimental results indicate that for this study, the ultimate failure was related to the tensile strength of the concrete rather than the FRP

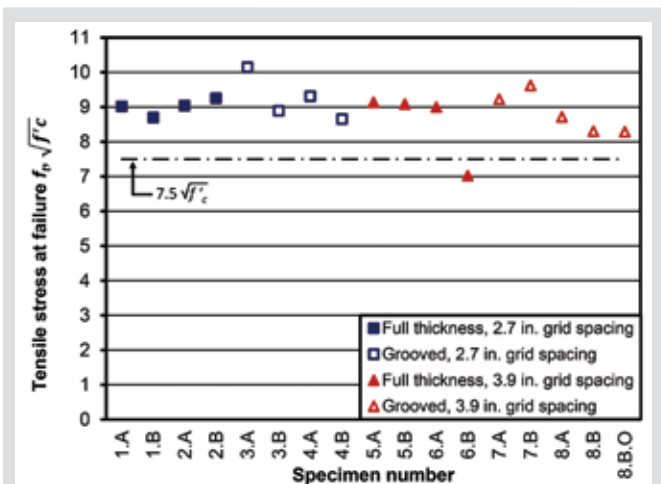


Figure 8. Tensile stress at failure f_b in terms of $\sqrt{f_c}$. Note: f_c is in psi. f_c = concrete compressive strength. 1 in. = 25.4 mm; 1 psi = 6.895 kPa.

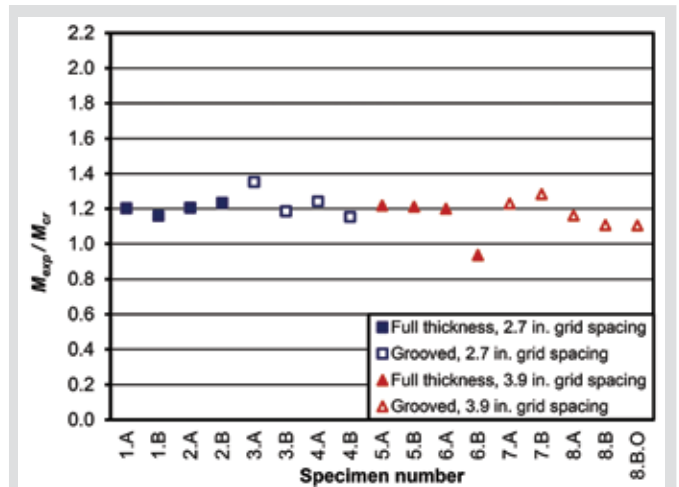


Figure 9. Ratio of measured moment at failure M_{exp} to predicted cracking moment M_{cr} . Note: 1 in. = 25.4 mm.

reinforcement ratio. Figure 9 compares the measured failure moment with the calculated cracking moment for all specimens.

$$M_{cr} = \frac{f_r b h^2}{6} \quad (2)$$

where

f_r = modulus of rupture = $7.5 \sqrt{f_c}$ psi ($0.62 \sqrt{f_c}$ MPa)

h = height of critical section

Design recommendations

Due to the brittle nature of the failure, it is recommended to use a strength-reduction factor ϕ of 0.75, similar to the factor used for shear failure of concrete structures. This recommendation differs from the strength-reduction factor of 0.55 provided by ACI 440.1R-06 for sections reinforced with FRP bars controlled by FRP rupture. The conservative value recommended by ACI 440.1R-06 is intended to prevent global failure in the event of rupture of the FRP bars.

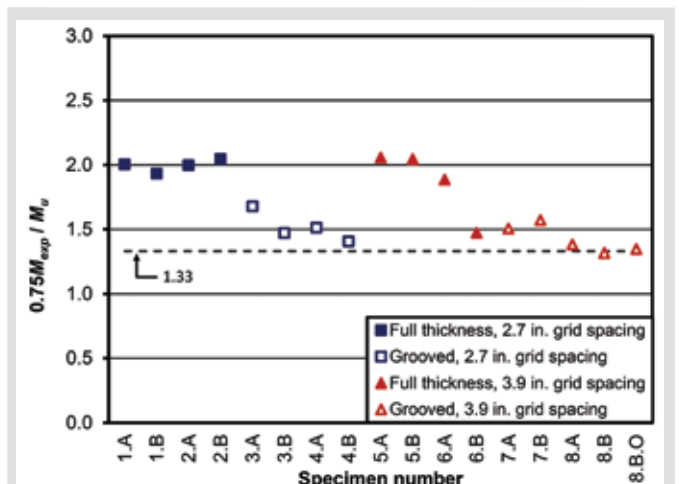


Figure 10. Ratio of reduced measured moment at failure M_{exp} to factored design moment M_r . Note: 1 in. = 25.4 mm.

However, CFRP grid reinforcement is believed to have a uniform distribution of the reinforcement and the failure of one strand will not result in global failure.

Given that in many cases the cracking moment M_{cr} exceeds the nominal flexural strength based on FRP rupture, it is recommended that the section be designed such that $0.75M_{cr}$ exceeds $1.33M_u$, where M_u is the ultimate moment due to applied factored loads (Eq. [3]). The ratio of $0.75M_{exp}$ (where M_{exp} is the measured moment at failure) is compared with M_u in **Fig. 10**, and nearly all tested specimens satisfied this recommendation. It is also recommended that the reinforcement be designed such that the reduced nominal flexural capacity $0.75M_n$ exceed the ultimate factored moment M_u (Eq. [4]).

$$0.75M_{cr} > 1.33M_u \quad (3)$$

$$0.75M_n > M_u \quad (4)$$

Design example

The following example illustrates a procedure for designing the FRP grid reinforcement for a precast concrete double tee. For a 3½ in. (90 mm) flange thickness, the dead load D is 43.75 lb/ft² (2.09 kPa). Using a live load L of 40 lb/ft² (2 kPa), and a snow load S of 20 lb/ft² (1 kPa), the controlling factored load is determined using Eq. (1).

For a flange cantilever length l of 3.11 ft (0.95 m), the factored ultimate moment under the given loading conditions is determined using Eq. (5):

$$\begin{aligned} M_u &= \frac{q_u l^2}{2} \quad (5) \\ &= \frac{(0.1265)(3.11)^2 (12)}{2} \\ &= 7.36 \text{ kip-in./ft (2.73 kN-m/m)} \end{aligned}$$

Select a 2.7 in. (70 mm) grid spacing, which is equivalent to 4.44 strands/ft (14.3 strands/m), and has rupture strength of 1.2 kip (5.3 kN) per strand. The design tensile strength of the FRP f_{fu} is 420 ksi (2900 MPa), the design rupture strain of the FRP ϵ_{fu} is 0.0123, and the area of FRP reinforcement A_f is 0.0127 in.²/ft (26.9 mm²/m). Using ¾ in. (19 mm) cover to the FRP, the effective depth d is 2.75 in. (70 mm). Given a design concrete strength in compression f'_c of 8000 psi (55,000 kPa), the FRP reinforcement ratio is determined from Eq. (8-2) and compared with the balanced reinforcement ratio from Eq. (8-3):

$$\rho_f = \frac{A_f}{bd}$$

$$= \frac{0.0127}{(12)(2.75)}$$

$$= 0.00039$$

$$\rho_{fb} = 0.85\beta_1 \frac{f'_c}{f_{fu}} \frac{E_f \epsilon_{cu}}{E_f \epsilon_{cu} + f_{fu}}$$

$$= 0.85(0.65) \left(\frac{8}{420} \right) \left[\frac{(34,000)(0.003)}{(34,000)(0.003) + 420} \right]$$

$$= 0.00206$$

Because the FRP reinforcement ratio is less than the balance ratio, Eq. (8-6b) and Eq. (8-6c), given previously from ACI 440.1R-06,³ are used to determine the moment capacity using a strength-reduction factor of 0.75. Equation (8-6b) is a conservative approach for determining the moment capacity, because the term $d - \frac{\beta_1 c_b}{2}$ is a lower bound of the moment arm. Some designers prefer to use the upper bound of the moment arm, which is simply the effective depth of the reinforcement d . However, this could lead to slightly unconservative results and should be used with caution.

$$c_b = \left(\frac{\epsilon_{cu}}{\epsilon_{cu} + \epsilon_{fu}} \right) d$$

$$= \left(\frac{0.003}{0.003 + 0.0123} \right) 2.75$$

$$= 0.539 \text{ in. (13.7 mm)}$$

$$M_n = A_f f_{fu} \left(d - \frac{\beta_1 c_b}{2} \right)$$

$$= (0.0127)(420) \left[2.75 - \frac{(0.65)(0.539)}{2} \right]$$

$$= 13.7 \text{ kip-in./ft (5.08 kN-m/m)}$$

$$\phi M_n = 0.75(13.7)$$

$$= 10.3 \text{ kip-in./ft (3.82 kN-m/m)}$$

The cracking moment is determined using Eq. (2) and compared with 1.33 times the factored ultimate moment. Because the moment capacity exceeds the demand and 0.75 times the cracking moment exceeds 1.33 times the factored ultimate moment from Eq. (5), the design is acceptable.

$$M_{cr} = \frac{f_r b h^2}{6}$$

$$= \frac{7.5 \sqrt{8000} (12) (3.5)^2}{6 (1000)}$$

$$= 16.4 \text{ kip-in./ft (6.09 kN-m/m)}$$

$$0.75M_{cr} = 0.75(16.4)$$

$$= 12.3 \text{ kip-in./ft (4.56 kN-m/m)}$$

$$1.33M_u = 1.33(7.36)$$

$$= 9.79 \text{ kip-in./ft (3.63 kN-m/m)}$$

Conclusion

This study indicates that the proposed precast concrete double-tee beams reinforced with CFRP grid are capable of resisting uniform pressures well in excess of the design loading. The mode of failure for these specimens was governed by the tensile strength of the concrete followed immediately by rupture of the CFRP grid. Application of sustained factored load did not influence the ultimate strength of the specimens nor did the sustained load significantly increase the deflection. It is recommended that a designer ensure that the reduced nominal flexural strength with a strength-reduction factor ϕ of 0.75 exceeds the moment due to factored load. It is also recommended to ensure that the reduced flange cracking moment capacity exceeds 1.33 times the moment due to factored load. Deflection of the flange should remain within the allowable limits specified by ACI 318-11 and ACI 440.1R-06. The double tees tested did not crack under service load.

Acknowledgments

The authors gratefully acknowledge the financial support of the National Science Foundation Industry and University Cooperative Research Center for Integration of Composites into Infrastructure. The authors would also like to thank AltusGroup Inc. for their support, including the donation of test specimens.

References

1. American Society of Civil Engineers (ASCE). 2010. *Minimum Design Loads for Buildings and Other Structures* (ASCE/SEI 7-10). Reston, VA: ASCE.
2. Lucier, G., J. McEntire, and S. Rizkalla. 2012. "Concentrated Load Tests of Precast Concrete Double-Tee Flanges Reinforced with CFRP Grid." Technical Report No. IS-12-20. Raleigh, NC: Constructed Facili-

ties Laboratory, Department of Civil, Construction, and Environmental Engineering, North Carolina State University.

3. American Concrete Institute (ACI) Committee 440. 2006. *Guide for the Design and Construction of Structural Concrete Reinforced with FRP Bars* (ACI 440.1R-06). Farmington Hills, MI: ACI.
4. ACI Committee 318. 2011. *Building Code Requirements for Structural Concrete* (ACI 318-11). Farmington Hills, MI: ACI.

Notation

A_f = cross-sectional area of FRP reinforcement

b = width of critical section

c_b = distance from extreme compression fiber to neutral axis at balanced strain condition as determined by Eq. (8-6c)

d = effective depth of reinforcement

D = design dead load

E_f = modulus of elasticity of FRP reinforcement

f_{fu} = rupture strength of FRP reinforcement

f_r = modulus of rupture

f_t = tensile stress at failure

f'_c = concrete compressive strength

h = height of critical section

l = flange cantilever length

L = design live load

M_{cr} = cracking moment

M_{exp} = measured moment at failure

M_n = nominal moment capacity

M_u = factored ultimate moment

P = measured pressure (including self-weight)

$P1$ = pressure outside testing chamber

$P2$ = pressure inside testing chamber

- P_a = applied pressure (excluding self-weight)
- P_{cr} = measured pressure at first crack (including self-weight)
- P_{exp} = measured failure pressure (including self-weight)
- q_u = factored design load
- S = design snow load
- β_1 = factor relating depth of equivalent rectangular compressive stress block to neutral axis depth specified by AC1318-11
- Δ = measured net deflection
- Δ_s = measured deflection under service load
- ϵ_{cu} = concrete crushing strain
- ϵ_{fu} = design rupture strain of FRP reinforcement
- ρ_f = FRP reinforcement ratio
- ρ_b = balanced FRP reinforcement ratio
- ϕ = strength-reduction factor

About the authors



Dillon Lunn, PhD, is a former postdoctoral scholar in the department of Civil, Construction, and Environmental Engineering at North Carolina State University (NCSU) in Raleigh, N.C. He is an engineering intern at Fluhrer Reed

Structural Engineers in Raleigh, North Carolina.



Gregory Lucier, PhD, is a research assistant professor at NCSU in the Department of Civil, Construction, and Environmental Engineering. He manages the NCSU Constructed Facilities Laboratory and specializes in large-scale

structural testing and research.



Sami Rizkalla, PhD, is a distinguished professor of Civil and Construction Engineering and the director of the Constructed Facilities Laboratory, NCSU. He is a fellow of PCI, the American Concrete Institute (ACI), the American Society of Civil

Engineers, the International Institute for FRP in Construction, the Engineering Institute of Canada, and the Canadian Society for Civil Engineering. He is also director of the National Science Foundation's Center of Integration of Composites into Infrastructure.



Ned Cleland, PhD, PE, is the president of Blue Ridge Design Inc. in Winchester, Va. He is a fellow of PCI and ACI. He has served on several PCI technical committees and councils, including the Seismic Committee,

Technical Activities Council, Parking Structures Committee, Building Code Committee, Research and Development Council, Industry Handbook Committee, and Professional Member Committee. At ACI, he has served on many committees, including ACI 318 Structural Concrete Building Code, ACI 362 Parking Structures, and ACI 550 Precast Concrete Structures.



Harry Gleich, PE, is vice president of engineering at Metromont Corp. He is a fellow of both PCI and ACI. He serves on many PCI committees, including the Technical Activities Council, and is the immediate past chair of the

Research and Development Council for PCI. At ACI he also serves on numerous committees, including ACI 362 Parking Structures, and is chair of ACI 550 Precast Concrete Structures.

Abstract

Fiber-reinforced polymer (FRP) grid has several advantages over traditional welded-wire reinforcement, including high strength, corrosion resistance, light weight, and ease of installation. This research evaluates the behavior of double-tee flanges reinforced with FRP grid and subjected to uniform gravity pressure to examine their serviceability and failure mode. This study demonstrates that precast concrete double-tee beams reinforced with FRP grid are capable of resisting uniform pressures well in excess of the design loading. The mode of failure for these specimens was governed by the tensile strength of the concrete, with concrete cracking followed immediately by rupture of the FRP grid. No cracking was observed under service loading. It is recommended that the reduced nominal flexural strength with a ϕ factor of 0.75 exceed the moment due to factored load and that the reduced cracking moment capacity exceed 1.33 times the moment due to factored load.

Keywords

FRP grid, uniform pressure, double-tee flange, design recommendations, vacuum chamber.

Review policy

This paper was reviewed in accordance with the Precast/Prestressed Concrete Institute's peer-review process.

Reader comments

Please address reader comments to journal@pci.org or Precast/Prestressed Concrete Institute, c/o PCI Journal, 200 W. Adams St., Suite 2100, Chicago, IL 60606. ¶